

DOUBLE-DIFFUSION BEHAVIOR BETWEEN PHOSPHORIC ACID COMPLEX  
SOLVENT AND ORGANIC COAGULANT AND THEIR INCORPORATION  
INTO CELLULOSE FILM

RUI XIONG, FAXUE LI and JIANYONG YU\*

*College of Textiles, Donghua University, Shanghai 201620, China*  
*\*Modern Textile Institute, Donghua University, Shanghai 200051, China*

*Received August 28, 2012*

The double-diffusion behavior between phosphoric acid complex solvent (PACS) and organic coagulant was evaluated. In addition, the properties and micro-structure of cellulose films regenerated in PACS and organic coagulants were investigated by scanning electron microscope (SEM), water contact angle (WCA), tensile test, X-ray diffraction (XRD), and fourier transform infrared spectroscopy (FTIR). SEM images demonstrated that the film prepared in ethanol/methanol exhibited a mostly non-uniform morphology mainly resulting from the highest double-diffusion rate during coagulation. The best hydrophobicity of the film prepared in ethanol/glycol, as determined by WCA measurements, was also better explained by the corresponding lowest double-diffusion rate. The cellulose solution seemed favored by ethanol/acetone to be processed into film with satisfactory mechanical properties and crystallinity, which was probably attributed to the neither too fast nor too slow double-diffusion rate. FTIR analysis confirmed that no drastic change occurred in the micro-structure of cellulose films irrespective of the coagulation bath.

**Keywords:** double-diffusion behavior, phosphoric acid complex solvent (PACS), cellulose film, coagulation, morphology, wettability, tensile strength

## INTRODUCTION

Dissolution of cellulose, one of the typical biopolymers in nature, in anhydrous phosphoric acid has been shown to occur quickly – in a matter of minutes – and can reach concentrations as high as 38%.<sup>1</sup> Anhydrous forms of phosphoric acid were obtained by adding tetraphosphoric acid (TPA, H<sub>6</sub>P<sub>4</sub>O<sub>13</sub>) to molten orthophosphoric acid (OPA, H<sub>3</sub>PO<sub>4</sub>), wherein the content of P<sub>2</sub>O<sub>5</sub> was greater than 74%. At a cellulose concentration above 7.5% in anhydrous phosphoric acid, liquid crystalline solutions are obtained, which can be wet spun into acetone to coagulate into fibers. Although the tensile properties of washed and neutralized fibers have been measured, their coagulation in ‘non-solvents’, accompanied by double - dispersion

between solvent and coagulator and regeneration of cellulose, has not been studied. Furthermore, the processing of cellulose-anhydrous phosphoric acid solutions into other forms, such as films, has not been explored.

Solvent ‘dispersion’ in wet spinning involves the diffusion between the solvent from wet fibers and the coagulant. Diffusion is a ubiquitous and fundamental process characterized by the haphazard motion of elementary constituents of matter – in this case, solvent molecules – due to thermal energy. An indispensable property in the diffusion process is the diffusivity or the diffusion coefficient. Research on diffusion coefficients has concerned mainly two areas. The first is the ‘self’

and ‘mutual’ diffusion coefficient. Self-diffusion coefficients were predicted by molecular dynamics simulations, which were also utilized to investigate the impact of particle roughness in granular gases on the self-diffusion,<sup>2</sup> as well as the Green-Kubo method.<sup>3</sup> The Taylor dispersion technique for mutual diffusion coefficients in binary systems,<sup>4</sup> electrochemical methods, coupled numerical models, water vapor absorption method, dynamic optical monitoring methods, numerical volume fraction models, molecular simulations and ‘multi-scale’ models for the diffusion coefficients of a single solute,<sup>5-11</sup> transient-state methods and also, the Taylor dispersion method for mutual diffusion coefficient of double component system,<sup>12,13</sup> and OSPR models, transient diffusion visualization by phase shifting techniques, molecular dynamic simulations and Maxwell-Stefan improved thermodynamic descriptions for multi-component systems<sup>14-17</sup> have been used to make predictions and compare with experimental data. The second is the ‘parameter-dependent’ diffusion coefficient, which is used to directly determine the concentration-<sup>18</sup> time-,<sup>19</sup> time/depth-,<sup>20</sup> or size-<sup>21</sup> dependent diffusion coefficients.

Processing cellulose into films and related composites is of great interest from both economic and environmental points of view. Films produced from bacterial cellulose have been studied for their mechanical<sup>22</sup> and anti-bacterial properties.<sup>23</sup> Cellulose films that have been processed from NaOH/thiourea solvents and mixed with chitosan exhibited limited biodegradability, increased surface roughness, and improved mechanical properties,<sup>24</sup> such as reduced brittleness.<sup>25</sup> Cellulose films have also been prepared from aqueous NaOH and related solutions,<sup>26</sup> ionic liquids,<sup>27</sup> or reinforced with nano-materials.<sup>28-30</sup>

In this work, the processing of cellulose from anhydrous phosphoric acid solutions into films was investigated. The double-diffusion behavior between phosphoric acid complex solvent (PACS) and organic coagulants, such as ethanol, a widely used coagulant for cellulose solutions,<sup>31-33</sup> as well as that of other coagulant mixtures, was evaluated and described by the mutual diffusion coefficient on the basis of a new binary-diffusion theory. The morphology, wetting and mechanical properties, as well as the micro-structure of cellulose films regenerated in PACS and the afore-mentioned organic solvents were characterized and analyzed by SEM, WCA, tensile test, XRD and FTIR

measurements.

## EXPERIMENTAL

### Materials

Cotton cellulose, with a degree of polymerization (DP) of 1000 (Xiangtai cell. Co., Ltd. Hubei, China) was dried at 65 °C in vacuum for 24 h and then stored over desiccant at ambient temperature when not in use. Aqueous solution of phosphoric acid (85% purity of H<sub>3</sub>PO<sub>4</sub>, orthophosphoric acid (OPA), 1.685 g/cm<sup>3</sup> density) and tetraphosphoric acid H<sub>6</sub>P<sub>4</sub>O<sub>13</sub> (TPA, 80% P<sub>2</sub>O<sub>5</sub> concentration, 2.0 g/cm<sup>3</sup> density) were supplied by Guoyao Reagent Co., Ltd. (Shanghai, China).

### Solvent preparation and cellulose dissolution

Anhydrous PACS were prepared by adding TPA to the aqueous solution of phosphoric acid at 43 °C, above the melting temperature of OPA, and stirring for 2 h to achieve a specific P<sub>2</sub>O<sub>5</sub> concentration and afford the hydrolysis of partial TPA to OPA. At 72.4% P<sub>2</sub>O<sub>5</sub>, the concentration of pure OPA was calculated from the formula weight ratio of P<sub>2</sub>O<sub>5</sub>/H<sub>3</sub>PO<sub>4</sub>. As the aqueous solution of phosphoric acid and TPA were added into the flask according to the given mass ratio of 0.62:1 between them, the PACS with P<sub>2</sub>O<sub>5</sub> concentration of 73% could be prepared and then stored at 0 °C for 24 h. The P<sub>2</sub>O<sub>5</sub> concentration of PACS was calculated by the following equation (1):

$$P_2O_5(\%) = \frac{0.62 \times 85\% \times 72.4\% + 1 \times 80\%}{0.62 + 1} = 73\% \quad (1)$$

After the hydrolysis of TPA to OPA, the actual mass proportion of TPA in PACS was determined to be 20.6% in theory in the homogeneous complex solvent.

A 10 L kneader was pre-cooled at 0 °C and charged with cellulose pulps and the prepared PACS at a w/w ratio of 17/83 cellulose-to-liquor. The mixture was agitated at 40 rad/min for a specific amount of time to prepare the cellulose solutions.

### Cellulose film preparation

Films were prepared from the cellulose/PACS solutions containing P<sub>2</sub>O<sub>5</sub> concentration of 73%. 1 g cellulose solution was spread on a glass slide and coagulated by immersing in one of the 220 g coagulants for 1 h at ambient temperature, as follows: pure ethanol, 1:1 w/w ethanol/acetone, 1:1 w/w ethanol/methanol and 1:1 w/w ethanol/glycol. The coagulated films were washed with distilled water to remove any remaining acid and dried under vacuum at 42 °C for 2 h.

### Recycling of coagulation bath

Each coagulation bath containing PACS and organic solvents was first poured into a separatory funnel with a filter sheet, and then the funnel was sealed to minimize moisture contamination and the liquor was filtered and gradually collected by a vacuumizing flask for 2 h. The

organic solvent was evaporated by heating the collected coagulation bath at 100 °C, and then it was condensed at 0 °C and successfully recycled. The 'residue' left on the filter sheet was dried in vacuum at 80 °C for 1 h then cooled at ambient temperature and stored over a desiccator.

## Characterization

### Viscosity measurements

The absolute viscosity of the coagulant was measured at 25 °C and 50% relative humidity using a NDJ-7 type rotary viscometer (Precision & Scientific Instrument Ltd. Co., Shanghai, China). A 15 mL specimen of each coagulant was degassed under vacuum for 15 min, and stored in a desiccator prior to performing the viscosity measurement. The range of absolute viscosity was varied from 1 to 10<sup>6</sup> mPa·s.

### Conductivity measurements

The conductivity coefficients of each coagulant ( $k_{st}$ ), as well as those containing PACS ( $k_{st}$ ), were measured using a DDS-310 conductivity apparatus (Dapu Instrument Ltd. Co., Shanghai, China). Selected coagulants and those incorporated with PACS were tested with a dipped platinum rod for more than 3 min until a constant value was observed.

### Dielectric constant measurements

The dielectric coefficients of the coagulants were measured using a QS30 high voltage-capacitance-electrical bridge apparatus (Yanggao Electrical Co., Shanghai, China) operating in the range of voltage of 0-499.9 kV and a maximum electric current of 30 mA. The dielectric constant  $\epsilon_m$  of each coagulant was obtained using Equation (2) as follows:

$$\epsilon_m = \frac{C_m}{C_v} \quad (2)$$

where  $C_m$  is the capacitance of the testing medium (ethanol and its mixed coagulants) and  $C_v$  is the capacitance of vacuum, equal to 60 pF (10<sup>-12</sup> F).

### Scanning electron microscope (SEM) measurements

The surface morphology of regenerated cellulose films was observed using a Hitachi S-3000N scanning electron microscope (SEM, Model S-3000N, Hitachi Co., Japan). The specimens were sputtered with gold/platinum for 60 s.

### Water contact angle (WCA) measurements

Water contact angles (WCA) of cellulose films were measured in air using a contact angle meter (Contact Angle System OCA 40, Data Physics Co., Germany). Three different measurements were performed in air using 12  $\mu$ L droplets of liquid water and the average is reported. The triplicate measurements yielded a variation of  $\pm 3^\circ$ .

### Tensile tests

The tensile properties of cellulose films were determined at 10 mm gauge length and 10 mm/min crosshead speed using an Instron-3365 tensile test machine (Libaoshangmao Co., Shanghai, China). Tensile strength, elongation at break and initial tensile modulus were calculated from the stress-strain curves of the cellulose film samples.

### X-ray diffraction measurements

The X-ray measurement of regenerated cellulose films were performed at room temperature on a D/MAX-2550 PC X-ray diffraction (XRD) instrument (RIGAKU Co., Japan). The output power of the generator was 18 kW, and Nickel-filtered Cu K $\alpha$  radiation was used. The XRD profiles were recorded in the 2 $\theta$  range of 5-50° at a scanning rate of 0.12 °/min.

### FTIR measurements

The regenerated cellulose films were measured by a NEXUS-670 Fourier transform infrared spectroscopy (FTIR) (Nicolet Co., America). The range of spectrum frequency was 4000-350 cm<sup>-1</sup>.

## RESULTS AND DISCUSSION

### Evaluation of double-diffusion behavior between PACS and organic coagulants

As 1 g cellulose solution cast on the glass slide is dipped into each 220 g organic coagulant, the mass of OPA in PACS is calculated by '1  $\times$  83%  $\times$  79.4%', which is equal to 0.66 g, and that of TPA in PACS is figured out to be 0.17 g. In that case, 2 g and 3 g cellulose solution contain 0.34 g and 0.51 g TPA, according to the theoretical mass ratio of 1:0.17, respectively.

Fig. 1 exhibits the relationship between the mass of undissolved acid in the coagulation bath and that of coagulating cellulose solution in the corresponding coagulation bath. Each mass of the undissolved acid in the coagulation bath is calculated from the weight of 'residue' therein. It mainly manifests that TPA is hardly dissolved and dispersed in any coagulant of ethanol/acetone, ethanol/methanol, ethanol/glycol, and ethanol when cellulose solution is coagulating, which is probably because of its significantly high viscosity at ambient temperature. Consequently, as PACS is immersed into coagulation bath, it is believed that double-diffusion between OPA and organic coagulants occurs, accompanied by separation and precipitation of TPA from PACS.

The double-diffusion behavior between PACS and coagulant is evaluated using the following

assumptions:

(1) the coagulating solution is considered a binary liquid system composed of PACS prepared at 73% P<sub>2</sub>O<sub>5</sub> as the ‘solute’ and the organic coagulant as the ‘solvent’;

(2) because the Debye-Huckel theory and the Osager-Falkenlagen equation only apply to low charge electrolyte solutions, the concentration of the PACS should be less than 0.1 mol/L for each 220 g coagulant;<sup>34,35</sup>

(3) H<sub>3</sub>PO<sub>4</sub> → H<sup>+</sup> + H<sub>2</sub>PO<sub>4</sub><sup>-</sup> is the dominant reaction in the OPA ionization;

(4) as the volumes of OPA and coagulant molecules are far smaller than those of macromolecular chains in cellulose with high degree of polymerization, those small molecules can easily and randomly double-diffuse among the gaps of cellulose molecular chains without limitation. Thus, small molecules of TPA are also easy to precipitate.

The free flow of the analyte from the sample medium to the collecting medium, namely the flow of the PACS from the cellulose solution to ethanol or other coagulants, is governed by Fick’s first law of diffusion:

$$J = -D \frac{dC}{dz} \quad (3)$$

where  $J$  is the molar flux of the analyte,  $\frac{dC}{dz}$  is the

concentration gradient, and  $D$  is the diffusion coefficient. In a multi-component liquid system, each component in the solution possesses its own self-diffusion coefficient  $D_i$ , which can be calculated by using the following expression:<sup>36,37</sup>

$$D_i = \frac{RTB_i}{x_i} \left(1 + \frac{\delta \ln \gamma_i}{\delta \ln x_i}\right) \quad (4)$$

where  $R$  and  $T$  are constants,  $B_i$  is the mobility term describing the transfer ability of the liquid and a positive constant,  $\gamma_i$  is the activity coefficient of species  $i$  in the mixture,  $x_i$  is the molar ratio of species  $i$ , and  $1 + \frac{\delta \ln \gamma_i}{\delta \ln x_i}$  is the thermodynamic factor

of species  $i$ .

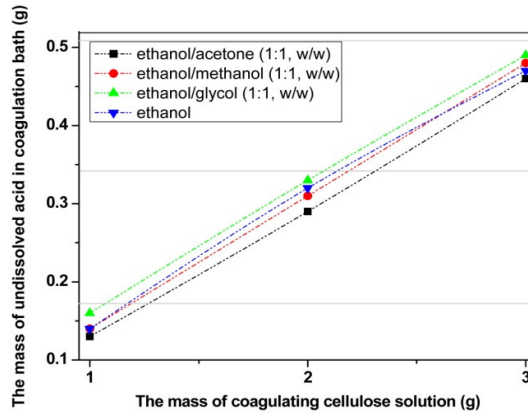


Figure 1: Mass of undissolved acid in coagulation bath versus that of coagulating cellulose solution therein

The activity coefficient  $\gamma$  is calculated first from modified Debye-Huckel theory and the Osager-Falkenlagen equation:

$$\lg \gamma_{\pm} = a(\lambda - \lambda_0) - \lg(1 + 0.001 \times v m M) \quad (5)$$

$$\text{where } a = \frac{A|Z_+ \cdot Z_-|}{B\lambda_0 + B_2} \quad (6)$$

$$A = \frac{1.8246 \times 10^6}{(\epsilon T)^{1.5}} \quad (7)$$

$$B_1 = \frac{2801 \times 10^6 |Z_+ \cdot Z_-| q}{(\epsilon T)^{1.5} (1 + \sqrt{q})} \quad (8)$$

$$B_2 = \frac{41.25 \times (|Z_+| + |Z_-|)}{\eta (\epsilon T)^{0.5}} \quad (9)$$

$$q = \frac{|Z_+ \cdot Z_-|}{|Z_+| + |Z_-|} \cdot \frac{L_+ + L_-}{|Z_-| L_+ + |Z_+| L_-} \quad (10)$$

$$\lambda = \frac{(k_{su} - k_{st}) \times 10^{-7}}{C} \quad (11)$$

where  $\gamma_{\pm}$  is the average activity coefficient of cations and anions in the solution,  $\lambda_o$  is the limiting molar conductivity ( $\text{S}\cdot\text{m}^2\cdot\text{mol}^{-1}$ ) of OPA in solution,  $\nu$  is the total number of cations and anions per molecule of OPA,  $m$  is the molality of OPA in the coagulating solution (mol/kg),  $M$  is the average molar mass of mixed coagulation reagents (g/mol),  $Z_+$  and  $Z_-$  are the charge numbers of the cation and anion, respectively,  $\varepsilon$  is the dielectric constant of the mixed coagulation reagents,  $\eta$  is the viscosity of the mixed coagulation reagents (mPa·s),  $L^{\circ}_+$  and  $L^{\circ}_-$  are the limiting molar conductivities of the cation and anion, respectively, and  $k_{su}$  and  $k_{st}$  are the conductivities of the solution and solvent ( $\mu\text{S}/\text{cm}$ ), respectively, wherein  $k_{st}$  of all organic coagulants was determined to be zero, and  $C$  is the molar concentration of the solution (mol/L).<sup>38</sup> Table 1 provides the values of  $\varepsilon$  and  $\eta$ . Under the assumptions presented,  $\gamma_{\pm}$  is approximately equal to the average activity coefficient  $\gamma$  of OPA in the solution, and  $|Z_+| = |Z_-| = 1$ .

Because  $\lambda$  is calculated by Equation (11) and provided in Table 1,  $\lambda_o$  can be extrapolated using  $\lambda \sim \sqrt{C}$ . Thus,  $a$  can be determined by Equation (6). Finally, each activity coefficient  $\gamma$  is obtained by Equation (5).

The Margules equation provides the relationship between the activity coefficient  $\gamma$  and the molar fraction  $x$  in a binary mixture<sup>39</sup> (wherein solute OPA is the species '1', and the coagulant as the

solvent is the species '2' in this binary system):

$$\ln \gamma_1 = x_2^2[A + 2x_1(B - A)] \quad (12)$$

where  $\gamma_1$  refers to the activity coefficient of the solute OPA,  $x_1$  and  $x_2$  refer to the molar fraction of OPA and the coagulation reagents in this mixture, respectively, and  $A$  and  $B$  are constants. To determine the values of  $A$  and  $B$ , we employ two groups of data from Table 1, conductivity with '0.83 g mass of PACS' and also '1.66 g mass of PACS'. Meanwhile, using Equation (4) we deduce the following expression for the diffusion coefficient of solute OPA:

$$D_1 = \frac{RTB_1}{x_1} \left(1 + \frac{\delta \ln \gamma_1}{\delta \ln x_1}\right) \quad (13)$$

Because  $R$ ,  $T$  and  $B_1$  are constants,  $D_1$  is determined from  $\frac{1}{x_1} \left(1 + \frac{\delta \ln \gamma_1}{\delta \ln x_1}\right)$ , where  $\frac{\delta \ln \gamma_1}{\delta \ln x_1}$  is the

partial derivative of  $\ln \gamma_1$  and  $\ln x_1$  in Equation (12). When immersing 1 g cellulose solution into different coagulation reagents, the values of  $\frac{1}{x_1} \left(1 + \frac{\delta \ln \gamma_1}{\delta \ln x_1}\right)$  in the characteristic diffusion

coefficients equation were calculated to be 640.6, 872.6, 624.2, 715.3 for 1:1 w/w ethanol/acetone, 1:1 w/w ethanol/methanol, 1:1 w/w ethanol/glycol and ethanol, respectively.

Table 1

Viscosity and dielectric constant of organic coagulants and molar conductivity of those containing the solute OPA with different molar concentrations

Organic coagulants	Viscosity (mPa·s)	Dielectric constant	Mass of PACS (g)	Molar concentration * 10 <sup>-2</sup> (mol/L)	Molar conductivity * 10 <sup>-8</sup> (S·m <sup>2</sup> ·mol <sup>-1</sup> )
ethanol/acetone (1:1, w/w)	1.0	782.5	0.83	2.4	4.2
			1.66	4.8	6.3
			2.49	7.2	7.0
ethanol/methanol (1:1, w/w)	0.7	427.1	0.83	2.4	8.3
			1.66	4.8	8.3
			2.49	7.2	8.3
ethanol/glycol (1:1, w/w)	2.7	50.4	0.83	2.8	3.5
			1.66	5.7	5.3
			2.49	8.5	5.9
ethanol	1.0	132.7	0.83	2.4	0
			1.66	4.8	1.4
			2.49	7.3	2.7

In a binary solution, the mutual diffusion coefficient  $D_{12}$  between the 'solute' and 'solvent',

as defined by Equation (14), can be used to describe the rate of double-diffusion between PACS

and organic coagulant because the driving force for mutual diffusion is the concentration gradient.<sup>40</sup>

$$D_{12} = x_1 D_2 + x_2 D_1 \quad (14)$$

In this extra-dilute ‘coagulation bath’ regime, when 1 g, 2 g, or 3 g cellulose solution is immersed into 220 g organic coagulants, the molar fraction of solute OPA ( $x_i$ ) in each coagulation bath is calculated to be less than 1%. In this case,  $D_{12}$  is approximately equal to  $D_1$ . As a result, the double-diffusion rate between PACS and coagulant of 1:1 w/w ethanol/methanol is the highest.

This simulation provides a qualitative and convenient method to evaluate the double-diffusion behavior between PACS at a fixed  $P_2O_5$  concentration of 73% and a variety of organic coagulants on account of their intrinsic properties, such as viscosity and dielectric constant, and provides profound insight into the regeneration of cellulose films or fibers for future applications. Under the same circumstances, the structure and properties of the consequent films regenerated from the solution with a fixed polymer content of 17% prepared by the incorporation of cellulose and PACS with  $P_2O_5$  concentration of 73% are chiefly affected by the organic coagulant, especially the surface morphology of the resulted films.

### Surface morphology of cellulose films

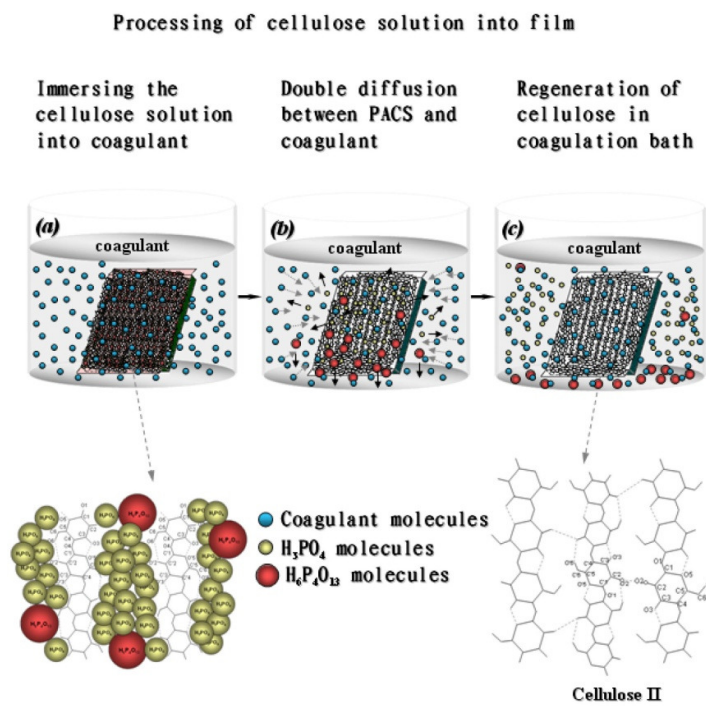
Scheme 1 describes the processing procedure for obtaining cellulose films. First, cellulose is dissolved in the PACS by reducing the intramolecular hydrogen bonding in cellulose through formation of phosphor-ester linkages.<sup>41</sup> After OPA and TPA molecules penetrate into the cellulose chains, the obtained homogeneous liquid solution provides the prerequisite for film preparation. Upon the double-diffusion between PACS and organic solvent with the precipitation of TPA during coagulation, cellulose loses its solubility and is gradually converted into a semisolid state, and then finally becomes regenerated from the original cellulose solution.<sup>42</sup> Fast regeneration of cellulose often leads to the formation of macro-voids on the surface of film, whereas a slow regeneration rate results in a denser structure.<sup>43</sup>

Fig. 2 shows the surface morphology of various regenerated cellulose films as characterized by SEM. There are large agglomerations and macro-voids on the surface of film (b) compared with that of films (a), (c), and (d). The non-uniform surface

morphology of film (b) likely resulted from the ‘too fast’ double-diffusion between solvent and non-solvent, as cellulose molecular chains have not sufficiently contacted with each other yet and are required to be precipitated from the coagulation bath. Some agglomerations are found on the surface of film (a) possibly due to the slightly inhomogeneous mutual diffusion between PACS and organic coagulant of 1:1 w/w ethanol/acetone caused by the relatively higher volatility of the acetone in comparison with other solvents, such as ethanol and glycol. It is noteworthy that both films (c) and (d), precipitated by the slower double-diffusion between PACS and coagulants, exhibit a comparatively smooth and dense morphology with a few particles on the surface. Therefore, in order to obtain regenerated cellulose films with uniform surface morphology, the double-diffusion rate during coagulation should be controlled to be as slow as possible, which is basically determined by the coagulation bath under the same circumstance.

### Wettability of cellulose films

The wettability of regenerated cellulose films is examined by measuring the contact angles of water droplet on the resulted films. It can be seen from Fig. 3 that all cellulose films prepared by the incorporation of cellulose solutions with organic solvents are characterized by moderate hydrophobicity. As the double-diffusion rate between PACS and organic solvents increases from the lowest for 1:1 w/w ethanol/glycol to the fastest for 1:1 w/w ethanol/methanol, there is a concurrent reduction in WCA on cellulose films from 74.2° to 58.6°. It is interesting to find that film (c), which is precipitated from 1:1 w/w ethanol/glycol, presents the best hydrophobic property with the highest water contact angle (WCA), compared to those of films (a), (b), and (d). This may correlate with the denser surface morphology, as shown in Fig. 2 (c). On the contrary, the water droplet seems to penetrate more easily into film (b) through its macro-voids on the surface. Therefore, film (b) exhibits the lowest WCA. In summary, the WCA results are mostly in agreement with the aforementioned phenomena and with the conclusions of SEM observation and evaluation of double-diffusion behavior between PACS and organic coagulants.



Scheme 1: Schematic illustration of processing cellulose solution into film

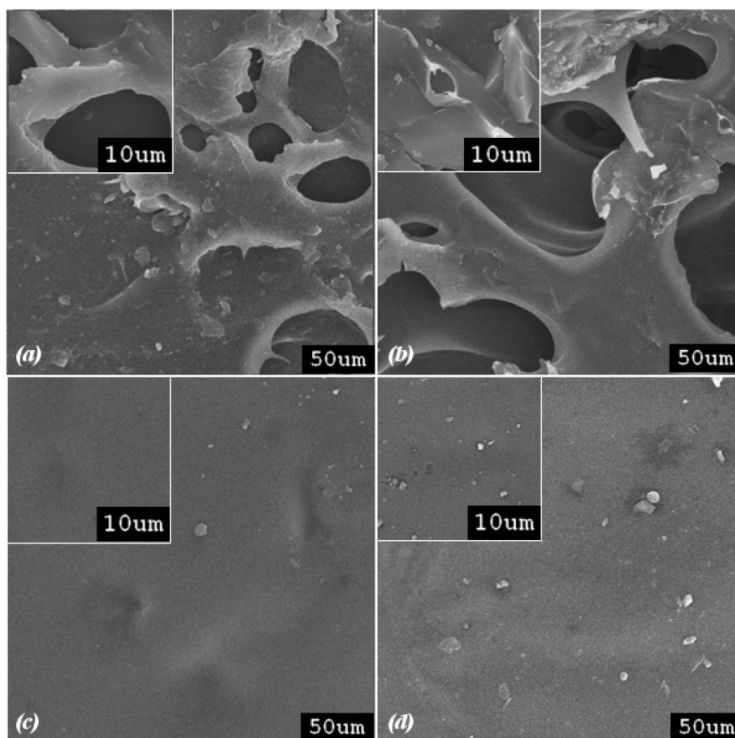


Figure 2: SEM micrographs of cellulose films precipitated from: (a) 1:1 w/w ethanol/acetone, (b) 1:1 w/w ethanol/methanol, (c) 1:1 w/w ethanol/glycol, and (d) ethanol

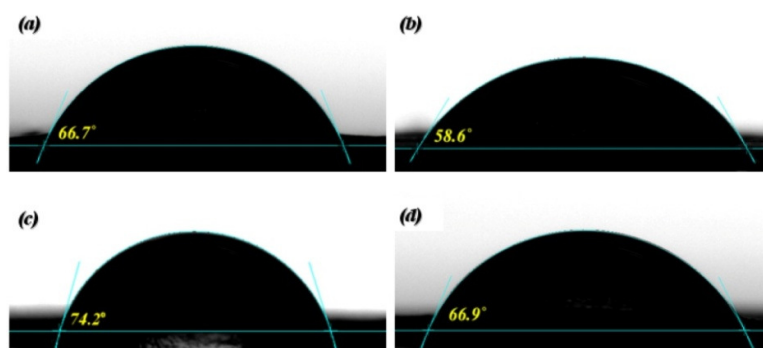


Figure 3: Water droplet on cellulose films precipitated from: (a) 1:1 w/w ethanol/acetone, (b) 1:1 w/w ethanol/methanol, (c) 1:1 w/w ethanol/glycol, and (d) ethanol

### Analysis of mechanical properties

The stress-strain curves of the regenerated cellulose films are provided in Fig. 4. The general linear shape of the curves indicates that all cellulose materials exhibit typical Hookean elasticity. It can be seen that the cellulose film precipitated from 1:1 w/w ethanol/acetone exhibits excellent mechanical properties with the highest tensile strength of 50 MPa, as well as the highest modulus of 893 MPa. 1:1 w/w ethanol/methanol and ethanol all render cellulose films with appreciably higher elongation at break, but remarkably lower tensile strength and modulus than 1:1 w/w ethanol/acetone. Combined with the results deduced in the ‘double-diffusion behavior between PACS and organic coagulants’ part, it implies that either too fast (1:1 w/w ethanol/methanol) or too slow (1:1 w/w ethanol/glycol) double-diffusion rate during coagulation will render the cellulose films with unsatisfactory mechanical properties. Cellulose solution seems favored by the organic coagulant of 1:1 w/w ethanol/acetone and can be processed into a rigid biomaterial.

### XRD analysis

The XRD spectra of regenerated cellulose films are shown in Fig. 5. The values of crystallinity are 40.5%, 29.8%, 34.4%, and 32.7% for the films precipitated from the coagulants of 1:1 w/w ethanol/acetone, 1:1 w/w ethanol/methanol, 1:1 w/w ethanol/glycol, and ethanol, respectively. The diffraction patterns of the resulted films exhibit three characteristic peaks at  $2\theta = 12.1^\circ$ ,  $20.0^\circ$ , and  $21.9^\circ$ , corresponding to the lattice plane of (101), (10 $\bar{1}$ ) and (002) in crystal structure of cellulose II, respectively.<sup>44,45</sup> These results reveal that the

relatively lower double-diffusion rate between PACS and 1:1 w/w ethanol/acetone than that between PACS and 1:1 w/w ethanol/methanol may currently supply a comparatively better environment to the regeneration of cellulose, which is beneficial for the gradual contact and recrystallization between molecular main chains of cellulose in the coagulation bath and also probably provides the corresponding cellulose film with relatively higher tensile strength and modulus, as discussed above. Besides, the relatively lower crystallinity of films prepared from 1:1 w/w ethanol/methanol and ethanol might bring better ductility to them, as presented and demonstrated by their slightly longer elongation at break in Fig. 4. This possibly resulted from the slippage among molecular chains, as well as their stretch in more amorphous regions of regenerated cellulose with lower crystallinity.

### FTIR analysis

Fig. 6 exhibits the FTIR spectra of cellulose films precipitated from various organic coagulants. Some characteristic bands related to the structure of cellulose II are the overlapped bands of hydroxyl group (-OH) in the regions  $3570\text{--}3450\text{ cm}^{-1}$  and  $3400\text{--}3200\text{ cm}^{-1}$ , attributed to intra- and intermolecular hydrogen bond of cellulose,<sup>46,47</sup> the band at around  $2900\text{ cm}^{-1}$ , whose main intensity comes from the C-H stretching vibrations,<sup>48</sup> the band at around  $1430\text{ cm}^{-1}$  due to the H-C-H and O-C-H in-plane bending vibration,<sup>49</sup> the bands in the region  $1200\text{--}970\text{ cm}^{-1}$  assigned to C-C (at about  $1200\text{ cm}^{-1}$ ) and C-O (at about  $993\text{ cm}^{-1}$ ) stretching vibration in the pyranose ring and C-O-C (at about  $898\text{ cm}^{-1}$ ) stretching of the glycosidic bonds, which

is common for all polysaccharides.<sup>50</sup>

As seen from the FTIR spectra of all resulted films, no drastic change occurs in the structure of regenerated cellulose irrespective of the coagulation bath. Because the relative intensity ratio of  $I_{4000-2995}/I_{993}$  could be applied as a criterion of hydrogen bond intensity,<sup>49</sup> the comparatively sharper peak

appeared in the cellulose film precipitated from ethanol at around  $993\text{ cm}^{-1}$  leads to the lowest intensity of hydrogen bond between molecular chains under the circumstance of nearly the same intensity of peaks appeared in the region  $4000\text{-}2995\text{ cm}^{-1}$  centered at around  $3300\text{ cm}^{-1}$  of all film specimens.

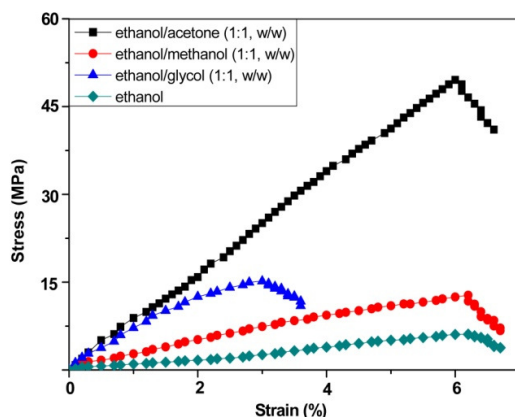


Figure 4: Stress-strain curves of cellulose films precipitated from different organic coagulants

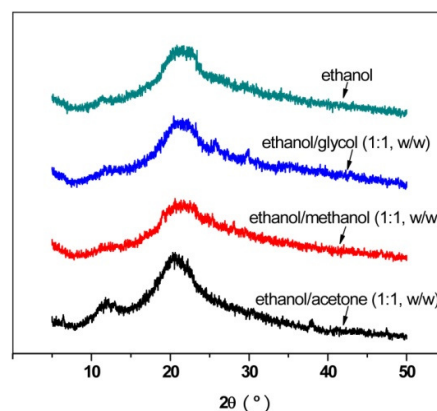


Figure 5: XRD spectra of cellulose films precipitated from different organic coagulants

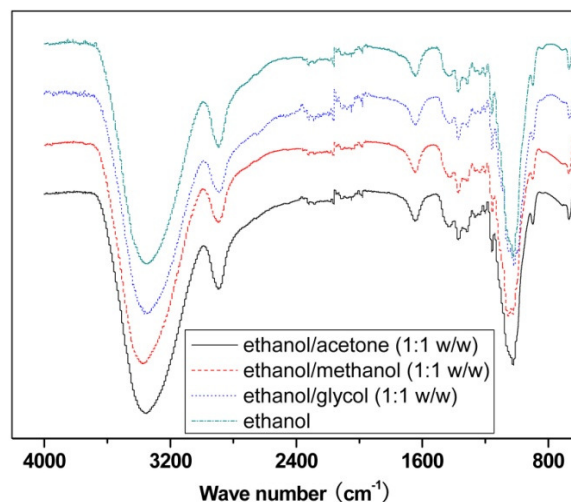


Figure 6: FTIR spectra of cellulose films precipitated from different organic coagulants

This might correlate with the regeneration mechanism of cellulose during coagulation in pure ethanol determined by its natural properties, such as viscosity, functional groups and so on.

## CONCLUSION

The double-diffusion behavior between PACS and organic coagulants was successfully described by the mutual diffusion coefficient in a binary solution during coagulation, and its effect on the

surface morphology, mechanical and wettability properties, as well as the micro-structure of regenerated cellulose films were also evaluated, which made it possible to perform detailed SEM and WCA characterization and provided profound insight into relevant processes for future. Tensile test results revealed that the cellulose film produced from a solution with 17/83 cellulose-to-liquor ratio prepared at 73%  $\text{P}_2\text{O}_5$  coagulating using 1:1 w/w ethanol/acetone exhibited the highest tensile strength and modulus, resulting in a rigid

biomaterial. Cellulose solution seemed favored by 1:1 w/w ethanol/acetone to be processed into film with predominant mechanical properties, as well as crystallinity, which mainly resulted from the moderate double-diffusion rate during coagulation. FTIR analysis illustrated that there was no remarkable change in the micro-structure of the resulted cellulose films in spite of the coagulation bath. Coagulation with pure ethanol rendered the film with relatively lower intensity of the hydrogen bond between cellulose chains, which seemed to result from the regeneration of cellulose during coagulation determined by the nature of ethanol. The processing of cellulose solutions to films was economical owing to the ease in recycling selected organic coagulants, which deserved to be considered as candidates for coagulation and regeneration of cellulose.

**ACKNOWLEDGEMENTS:** This work has been financially supported by the Fundamental Research Funds for the Central Universities, to which the authors express their gratitude.

## REFERENCES

- <sup>1</sup> H. Boerstael, H. Maatman, J. B. Westerink and B. M. Koenders, *Polymer*, **42**, 7371 (2001).
- <sup>2</sup> A. Bodrova and N. Brilliantov, *Granul. Matter.*, **14**, 85 (2011).
- <sup>3</sup> G. Guevara-Carrion, J. Vrabec and H. Hasse, *J. Chem. Phys.*, **134**, 074508 (2011).
- <sup>4</sup> M. H. Wang, A. N. Soriano, A. R. Caparanga and M. H. Li, *Journal of Taiwan Institute of Chemical Engineers*, **41**, 279 (2010).
- <sup>5</sup> T. Murakami and T. Koyama, *J. Electrochem. Soc.*, **158**, 147 (2011).
- <sup>6</sup> T. D. Myles, A. M. Kiss, K. N. Grew, A. A. Peracchio, G. J. Nelson and W. K. S. Chiu, *J. Electrochem. Soc.*, **158**, 790 (2011).
- <sup>7</sup> A. H. J. Paterson and G. Ripberger, *Proc. Food Sci.*, **1**, 1924 (2011).
- <sup>8</sup> A. L. Bychkov, S. M. Korobeynikov and A. Y. Ryzhkina, *Tech. Phys.*, **56**, 421 (2011).
- <sup>9</sup> M. Felberbaum, E. Landry-Desy, L. Weber and M. Rappaz, *Acta Mater.*, **59**, 2302 (2011).
- <sup>10</sup> M. Garcia-Rates, De H. Jean-Charles, J. B. Avalos and C. Nieto-Draghi, *J. Phys. Chem.*, **116**, 2787 (2012).
- <sup>11</sup> G. W. Sun, W. Sun, Y. S. Zhang and Z. Y. Liu, *J. Mater. Civ. Eng.*, DOI: 10.1061/(ASCE) MT.1943-5533.0000477 (2012).
- <sup>12</sup> H. Davarzani, M. Marcoux, P. Costeseque and M. Quintard, *Chem. Eng. Sci.*, **65**, 5092 (2010).
- <sup>13</sup> M. Toriumi, R. Katooka, K. Yui, T. Funazukuri, C. Y. Kong and S. Kagei, *Fluid Phase Equilib.*, **297**, 62 (2010).
- <sup>14</sup> S. A. Mirkhani, F. Gharagheizi and M. Sattari, *Chemosphere*, **86**, 959 (2012).
- <sup>15</sup> A. Komiya, J. F. Torres, J. Okajima, S. Moriya, S. Maruyama and M. Behnia, *2010 14<sup>th</sup> International Heat Transfer Conference*, 2010, CDROM IHTC-22501, vol. **2**, p. 555.
- <sup>16</sup> J. H. Yoo, A. Breitholz, Y. Iwai and K. P. Yoo, *Korean J. Chem. Eng.*, **28**, 1025 (2011).
- <sup>17</sup> S. Rehfeldt and J. Stichlmair, *Fluid Phase Equilib.*, **290**, 1 (2010).
- <sup>18</sup> A. E. Amooghin, H. Sanaeepur, A. Kargari and A. Moghadassi, *Sep. Purif. Technol.*, **82**, 102 (2011).
- <sup>19</sup> M. D. Prange, V. Druskin, D. L. Johnson and L. M. Schwartz, *J. Phys. A*, **44**, 1 (2011).
- <sup>20</sup> Y. M. Sun, T. P. Chang and M. T. Liang, *J. Mar. Sci. Technol.*, **19**, 660 (2011).
- <sup>21</sup> S. Zhang, *Adv. Mater. Res.*, **391-392**, 418 (2012).
- <sup>22</sup> A. Retegi, N. Gabilondo, C. Pena, R. Zuluaga, C. Castro *et al.*, *Cellulose*, **17**, 661 (2010).
- <sup>23</sup> B. Wei, G. Yang and F. Hong, *Carbohydr. Polym.*, **84**, 533 (2011).
- <sup>24</sup> D. L. Morgado, E. Frollini, A. Castellan, D. S. Rosa and V. Coma, *Cellulose*, **18**, 699 (2011).
- <sup>25</sup> E. V. R. Almeida, E. Frollini, A. Castellan and V. Coma, *Carbohydr. Polym.*, **80**, 655 (2010).
- <sup>26</sup> Q. L. Yang, H. Fukuzumi, T. Saito, A. Isogai and L. Zhang, *Biomacromolecules*, **12**, 2766 (2011).
- <sup>27</sup> Q. L. Yang, X. Z. Qin and L. Zhang, *Cellulose*, **18**, 681 (2011).
- <sup>28</sup> A. Takegawa, M. A. Murakami, Y. Kaneko and J. I. Kadokwa, *Carbohydr. Polym.*, **79**, 85 (2010).
- <sup>29</sup> E. Karabulut and L. Wagberg, *Soft Mater.*, **7**, 3467 (2011).
- <sup>30</sup> M. He, C. Y. Chang, N. Peng and L. Zhang, *Carbohydr. Polym.*, **87**, 2512 (2012).
- <sup>31</sup> R. Gavillon and T. Budtova, *Biomacromolecules*, **8**, 424 (2007).
- <sup>32</sup> R. Gavillon and T. Budtova, *Biomacromolecules*, **9**, 269 (2008).
- <sup>33</sup> Y. Mao, J. P. Zhou, J. Cai and L. Zhang, *J. Membrane Sci.*, **279**, 246 (2006).
- <sup>34</sup> M. A. Estes, O. M. Gonzalez-Diaz, F. F. Hernandez-Luis and L. Fernandez-Merida, *J. Sol. Chem.*, **18**, 277 (1989).
- <sup>35</sup> T. H. Lilley and C. C. Briggs, *Proc. Royal Soc.*, **349**, 355 (1976).
- <sup>36</sup> H. A. Kooijman and R. Taylor, *Ind. Eng. Chem. Res.*, **30**, 1217 (1991).
- <sup>37</sup> H. Strathmann and K. Kock, *Desalination*, **21**, 241 (1977).
- <sup>38</sup> E. Saljoughi, M. Amirilargani and T. Mohammadi, *J. App. Polym. Sci.*, **111**, 2537 (2009).
- <sup>39</sup> B. J. Zwolinski, H. Eyring and C. E. Reese, *J. Phys. Chem.*, **53**, 1426 (1949).
- <sup>40</sup> A. Vignes, *Ind. Eng. Chem. Fund.*, **5**, 189 (1966).

- <sup>41</sup> G. Butera, C. D. Pasquale, A. Maccotta, G. Alonzo and P. Conte, *Cellulose*, **18**, 1499 (2011).
- <sup>42</sup> A. Lopes, F. Farelo and M. I. A. Ferra, *J. Sol. Chem.*, **28**, 117 (1999).
- <sup>43</sup> J. H. Pan, W. Hamad and S. K. Straus, *Macromolecules*, **43**, 3851 (2010).
- <sup>44</sup> H. P. Fink and B. Philipp, *J. App. Polym. Sci.*, **30**, 3779 (1985).
- <sup>45</sup> L. Segal, M. L. Nelson and C. M. Conrad, *J. Phys. Chem.*, **55**, 352 (1951).
- <sup>46</sup> E. Samio, R. K. Dark and J. V. Dawkins, *Polymer*, **38**, 3045 (1997).
- <sup>47</sup> D. Fengel and M. Ludwig, *Papier*, **45**, 45 (1991).
- <sup>48</sup> J. Lojewska, P. Miskowiec, T. Lojewski and L. M. Proniewicz, *Polym. Deg. Stabil.*, **88**, 512 (2005).
- <sup>49</sup> S. Y. Oh, D. I. Yoo, Y. S. Shin and G. Seo, *Carbohydr. Res.*, **340**, 417 (2005).
- <sup>50</sup> A. Pielesz and W. Binias, *Carbohydr. Res.*, **345**, 2676 (2010).